Spatial and temporal pattern of extreme temperature during 1961–2018 in China

Xiaowan Liu and Zongxue Xu

ABSTRACT

As extreme climate events in China occur frequently, the characteristics of temperature extremes have changed substantially. Spatial and temporal pattern in the selected temperature extreme indices was analyzed by using the Mann–Kendall method (MK), sliding t-test and standard t-test, and Pearson correlation analysis method. In addition, the relationship between them and AO/NAO (Arctic Oscillation/North Atlantic Oscillation) was investigated during 1961–2018 in mainland China. The results show regional and seasonal pattern in temperature extremes. Both ELTs (extreme low temperatures) and EHTs (extreme high temperatures) show increasing trend in autumn and winter, but decreasing trend in spring and summer. In particular, ELTs in all northern basins have more significant increasing trend, while EHTs in the southern areas show insignificant or even decreasing trend. The AO plays an important role in the change of ELTs in summertime (summer and autumn), while the NAO accounts for it during wintertime (winter and spring). Moreover, the NAO is partly responsible for the change of EHTs.

Key words | Arctic Oscillation, China, frozen days, North Atlantic Oscillation, temperature extremes, Yangtze River

Xiaowan Liu (corresponding author)
Zongxue Xu
College of Water Sciences,
Beijing Normal University,
Beijing 100875,
China
and
Beijing Key Laboratory of Urban Hydrological Cycle and Sponge City Technology,
Beijing 100875,
China
E-mail: *xiaowan@mail.bnu.edu.cn*

INTRODUCTION

Extreme climate events have varied substantially over the last 60 years with identified regional differences (Cropper & Hanna 2012; Grant 2017; Mahmood & Jia 2017; Partal 2017). As a country that experiences serious climate extreme events and disasters, China is characterized by a variety of events with high frequency, obvious periodicities and seasonality, demonstrating significant regional discrepancy that encompasses a broad spectrum of impacts, such as frequent occurring heat waves, droughts, cold waves, and frost during the last few decades (López-Moreno *et al.* 2011; Jia *et al.* 2017). Temperature extremes are causations in extreme climate events, for which a significant trend has been widely observed in the last 60 years (Castro-Díez *et al.* 2002; You *et al.* 2013). Relevant studies (Frich *et al.* 2002; Fischer *et al.* 2011; You *et al.* 2013) have indicated that these hydrological extreme events are directly correlated with climate extreme events. Precipitation was also found to have a close relationship with temperature, while the relationship differs from region to region (Beniston & Rebetez 1996; Gruza *et al.* 1999; New *et al.* 2006; Li *et al.* 2011). In addition, the linkage of vegetation growth to temperature changes has been widely studied. It has been acknowledged that vegetation degradation is related to change in temperature extremes (Meehl *et al.* 2000; Sun & Wang 2008; Wang *et al.* 2010). Therefore, furthering the understanding on climatic extremes is essential to predict future hydrological changes and provide a reference for water resources management and ecological protection (Mutiibwa *et al.* 2015).

A large number of studies has investigated the spatial and temporal pattern of temperature extremes over the whole of China and individual basins (Jiang *et al.* 2011;

doi: 10.2166/wcc.2019.302

Zhang *et al.* 2012; Chen & Sun 2015; Su *et al.* 2017). The results generally show that change in temperature extremes during the past decades has been consistent with global warming. Tong *et al.* (2019) documented that extreme climate events became more frequent and have intensified generally since the last mid-century, while the frequent occurrence of such events in most parts of northern China started from the 1990s (Ma *et al.* 2003). On the other hand, the reason for temperature extremes in China has also been broadly explored, for which atmospheric circulation factors including NAO (North Atlantic Oscillation) and AO (Arctic Oscillation) were frequently combined (Chan & Zhou 2005; Suo *et al.* 2008; Wan *et al.* 2010; Zhou & Wu 2010; Renom *et al.* 2011; Wu & Qian 2015). For instance, Chen *et al.* (2016) pointed out that the AO is a primary factor that influences temperatures north of China, and the East Asian trough is considered to be a prime channel of influence (Lee & Zhang 2011; Shi *et al.* 2018). NAO was also hypothesized to be the main factor exerting significant impacts on the occurrence of cold surges south of China (Linderholm *et al.* 2013; Zuo *et al.* 2016). Extreme temperatures in East Asia were linked to the AO (He & Wang 2016), and the NAO correlated with frost days and cold days (Scaife *et al.* 2008). Wei & Lin (2009) found that negative phase in the AO could result in more frequent cold extremes in China, and vice versa.

Change in temperature extremes could significantly affect local natural water resources condition by hydrological cycle elements such as evapotranspiration, precipitation, runoff, etc. (Wang *et al.* 2015; Grant 2017; Ghorbani *et al.* 2018; Liu *et al.* 2018). Understanding spatial and temporal pattern in temperature extremes is fundamental to predict future water resources. However, the existing studies are quite discrete and rarely consider the water resources partition. To adapt to the regionalization mode in water resources management, this study was conducted based on the ten water resource subregions in mainland China (the map will be provided in the following part), considering each has a particular water resource condition with a corresponding climate. The aim of the present study is to investigate spatiotemporal patterns of temperature extremes and their relationship with the AO/NAO in the period of 1961–2018 based on the selected ten water resources regions. Islands are excluded from this study due to a lack of observational data.

DATA AND METHODOLOGY DESCRIPTIONS

Daily minimum and maximum temperature from 1961 to 2018 archived by the China Meteorological Data Service Center (http://data.cma.cn/) for 589 meteorological stations across mainland China was used for the analysis. Daily and monthly NAO index records covering the same period were obtained from the Climate Prediction Center (http://www.cpc.ncep.noaa.gov/). Seasonal values were averaged from monthly records, and the seasons were divided as follows: spring (March–May), summer (June–August), autumn (September–November), and winter (December–February). The selected extreme temperature indices include seasonal ELTs (extreme low temperatures), seasonal EHTs (extreme high temperatures), seasonal DTR (diurnal temperature range), and frozen days, frost days, and GSL (growing season length) on annual scale. Figure 1 shows the locations of the 589 meteorological stations and ten water resources regions.

According to the statistics, the area of the northwest rivers is over 36% (3.61×10^6 km^2) of the total area in mainland China, while only 17% (100 stations) of all selected stations are located in this area. The area of the Yangtze River basin is around 1.8×10^6 km^2, which accounts for 18% of the total area in mainland China, and 24% (139 stations) of all the selected stations are distributed in this area. The area in each of the residual basins is less than 10% of the total area in mainland China, particularly for the southwest rivers, where the area occupies 9% of the total area in mainland China while less than 6% (33 stations) of all stations are situated. In the following, northern areas contain the Songhua River, northwest rivers, Liaohe River, Haihe River, and Yellow River basin, and the Yangtze River, Huaihe River, southeast rivers, southwest rivers and Pearl River basin are marked as southern areas.

The Mann–Kendall non-parameter test (MK method) (Cropper & Hanna 2012), which analyzes trends, is utilized to detect the trend of extreme temperatures. In addition, to identify change points and significance, the sliding t-test and the standard t-test were simultaneously used (Waliser

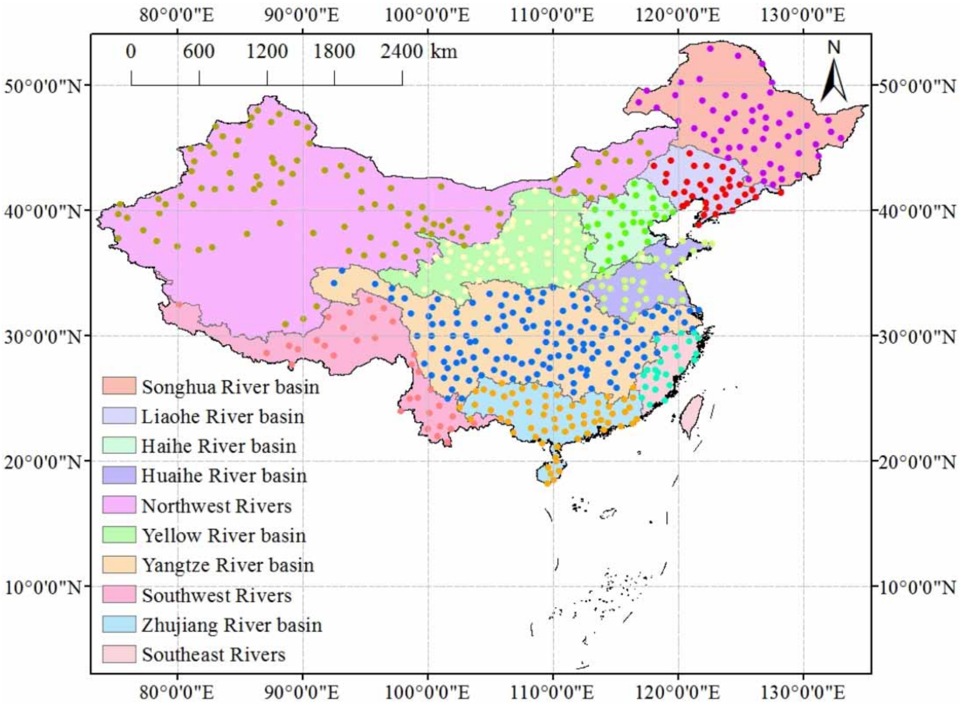

Figure 1 | Locations of 589 meteorological stations and ten water resources regions.

et al. 2003). Moreover, the Pearson correlation analysis (Donges *et al.* 2009) was also employed to analyze the relationship between AO/NAO and temperature extremes, and the t-test was used to verify the significance.

ANALYSIS OF THE RESULTS

Spatial patterns in temperature extremes in ten water resources regions

The spatial patterns of temperature extremes were analyzed using statistical methods, and the results are shown in Figure 2. The highest number of frozen days (118) occurred in the Songhua River basin, while the northwestern rivers and the Liao River basin have similar numbers of frozen days (approximately 70). Additionally, approximately 35–40 frozen days were observed in both the Yellow River and the Haihe River basins, while the southwestern rivers only experience 13 frozen days, 7 frozen days for both the Huai River and the Yangtze River basins, respectively. In addition, no frozen days appear in the southeastern rivers or in the Pearl River basin.

Similar to frozen days, the highest number of frost days (193) was also found in the Songhua River basin, and the number of frost days for the northwestern rivers is less (176 days). In addition, the number of frost days in the Liao River and Yellow River basins are similar (155–160). For the most southern basin in the northern region, i.e., the Haihe River basin, slightly fewer frost days (134) were observed. For the southern areas, over 100 frost days were observed in the southwestern rivers, while other basins have fewer than 100 frost days, as only 16 and 2 frost days occur in the southeastern rivers and the Pearl River basin, respectively.

The spatial pattern of the GSL is almost opposite that for frozen days and frost days; fewer frozen or frost days correspond to a longer GSL. To be specific, the shortest GSL occurs in the Songhua River basin (166 days), and the northwestern rivers have the second fewest number of days in the GSL (182). However, the anomaly is that both the number of frozen days and the GSL in the Liao River basin are greater than those in the Yellow River basin. In addition, in the Haihe River basin, a slightly longer GSL (226 days) was observed. Moreover, in increasing order, the GSLs of the southern areas can be listed as follows: the southwestern

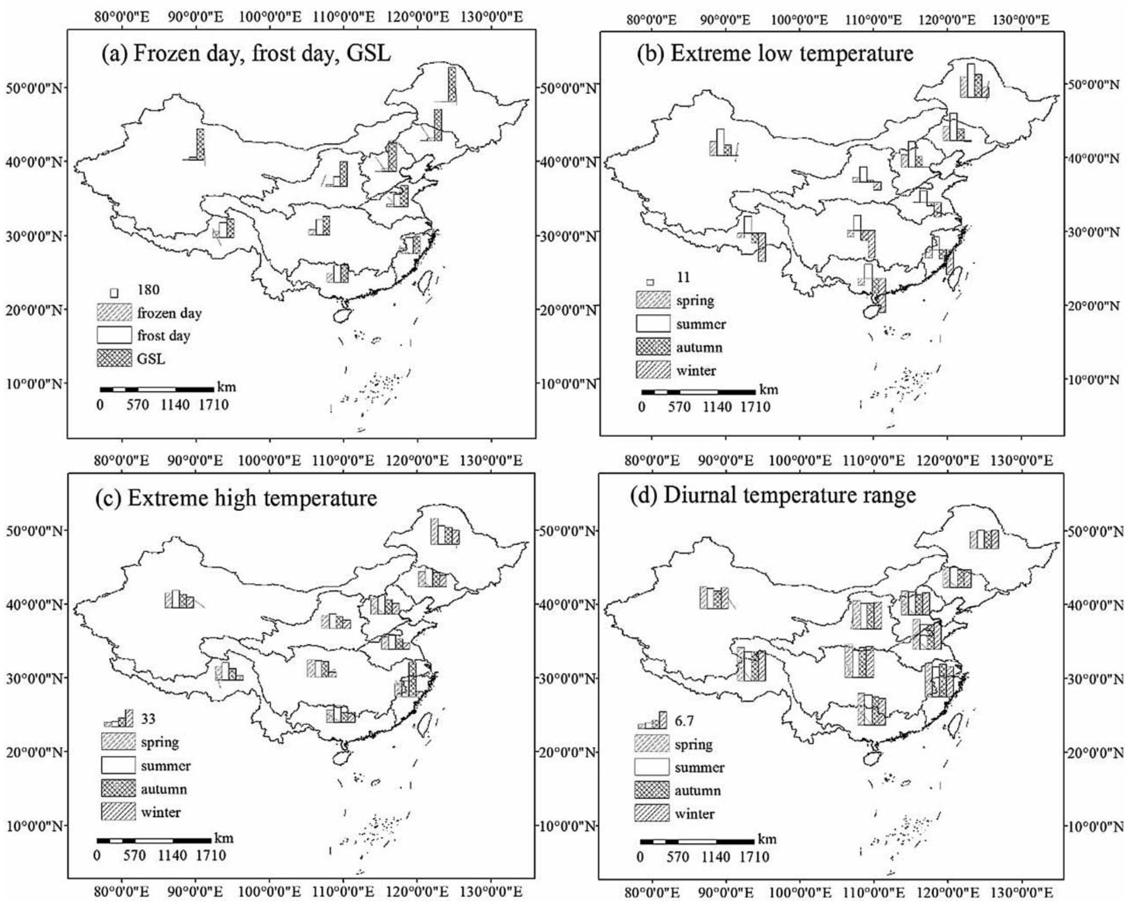

Figure 2 | Distribution of temperature extremes in ten water resources regions.

rivers, the Huai River basin, the Yangtze River basin, the southeastern rivers, and the Pearl River basin.

To detect the seasonality in temperature extremes, seasonal ELTs and EHTs were extracted for further analysis. The results show that the seasonal ELTs over northern areas are negative (below 0 °C), while the seasonal ELTs are positive (above 0 °C) over southern areas. Seasonally, spring ELTs are similar to those in autumn and lower than those in winter. Winter ELTs are negative except for those in the Pearl River basin, and all summer ELTs are positive. The lowest EHT reaches −30 °C in winter in the Songhua River basin, and the largest ELT (20 °C) occurs during summer in the Pearl River basin. Aside from the anomaly between the Liao River basin and the Yellow River basin, ELTs generally increase from north to south for each season. For the seasonal EHTs in the ten water resources regions, the values are positive. In comparison with the ELTs, the values between spring and autumn that are found in each water resources region are similar, while spring EHTs are slightly greater than those in winter. Lastly, for the DTR, the values in the northern areas are generally larger than those in the southern areas, particularly in the Huai River and Yangtze River basins. The southeastern rivers and the Pearl River basin have seasonal DTRs that are less than 10 °C in all seasons. The largest DTR (over 30 °C) occurs during autumn in the Haihe River basin.

Trend in temperature extremes in the ten water resources regions

To determine the trend in temperature extremes, the MK method was applied, and the results are shown in the supplementary material, Table S1. For the northern water resources regions, all seasonal ELTs have a clear increasing trend at 0.01 significance level, and an upward trend in autumn ELTs was observed only in the Liao River basin (at 0.05 significance level). For the southern water resources regions, all wintertime ELTs have an increasing trend at 0.01 significance level. In autumn, the ELTs across all southern water resources regions have an apparent upward trend at 0.05 significance level, and those in the Yangtze River and Huai River basins pass the 0.01 significance level test. Spring ELTs in all water resources regions show an upward trend, such that a majority pass the 0.01 significance level test. However, that of the Pearl River basin only passes the 0.05 significance level test and that of the southeastern river is nonsignificant. However, for the summertime ELTs, the southeastern rivers and the Pearl River basin have significantly decreasing and increasing trend respectively, while the other water resources regions show no apparent trend.

The trend in EHTs is not as significant as that for ELTs. Specifically, for the northern water resources regions, only the autumn and winter EHTs were identified as having significant trend (excluding those of the Songhua River and the Haihe River basins). In addition, the southwestern rivers show significant increasing trend in their seasonal EHTs. Both the winter EHTs in the Yangtze River basin and the summer EHTs in the Pearl River basin have distinguishable increasing trend at 0.01 significance level. Surprisingly, in the southeastern rivers, all the seasonal EHTs have decreasing trend at 0.05 significance level in spring and autumn and at 0.01 significance level in summer.

The DTR generally has a decreasing trend, particularly over the Songhua River basin and the northwestern rivers, which have trend at 0.01 significance level. In the Liao River and Haihe River basins, the seasonal DTR exhibits a decreasing trend at 0.01 significance level (excluding the summer DTR). In addition, the Yellow River basin has a significant decreasing trend for DTR in summer and winter at 0.01 significance level. In the southern water resources regions, all the winter DTRs have decreasing trend at 0.01 significance level in the southwestern rivers, southeastern rivers, and the Pearl River basin, while those in the Yangtze River and Huai River basins only pass the 0.05 significance level test. The summer DTRs in the Huai River basin, the Yangtze River basin, and the southeastern rivers show decreasing trend at 0.01 significance level. Moreover, the autumn DTRs in the Huai River basin, the southeastern rivers, and the Pearl River basin show decreasing trend; the former two basins pass the 0.01 significance level test, and the latter only passes the 0.05 significance level test. In terms of spring DTRs, the southwestern rivers and the Huai River and Pearl River basins have decreasing trend, but only the former passes the 0.01 significance level test, while the latter only pass the 0.05 significance level test.

In terms of the trend in frozen days, frost days, and the GSL, both frozen and frost days exhibit significant decreasing trend (excluding the frozen days in the Pearl River basin, which are nonsignificant). In addition, the trend in frozen days over the Huai River and Liao River basins only pass the 0.05 significance level test, while other water resources regions have increasing trend at 0.01 significance level for frozen and frost days. In addition, the GSL has an increasing trend at 0.01 significance level (except in the southeastern rivers). This increase in GSL may contribute to enhanced crop yields by providing opportunities for earlier planting, guaranteeing maturation, and the possibility of multiple cropping (Linderholm 2006).

Relationship between the AO/NAO and temperature extremes in ten water resources regions

The results of the correlation coefficients between the winter AO/NAO and temperature extremes and their significance level are shown in Figures 3(a)–3(f) and 4(a)–4(c) show the change points in temperature extremes when comparing with the winter AO/NAO. For the relationship between seasonal ELTs and the winter AO/NAO, the winter AO is closely related to the spring ELTs in the Songhua River, Liao River, and Haihe River basins and the southwestern rivers with relationships at 0.05 significance level. With respect to the winter NAO and seasonal ELTs, all basins have similar positive relationships of their winter NAO and spring ELTs at 0.01 significance level, especially in the Songhua River, Yellow River, Haihe River, Yangtze River, Huai River, and Pearl River basins and the southwestern

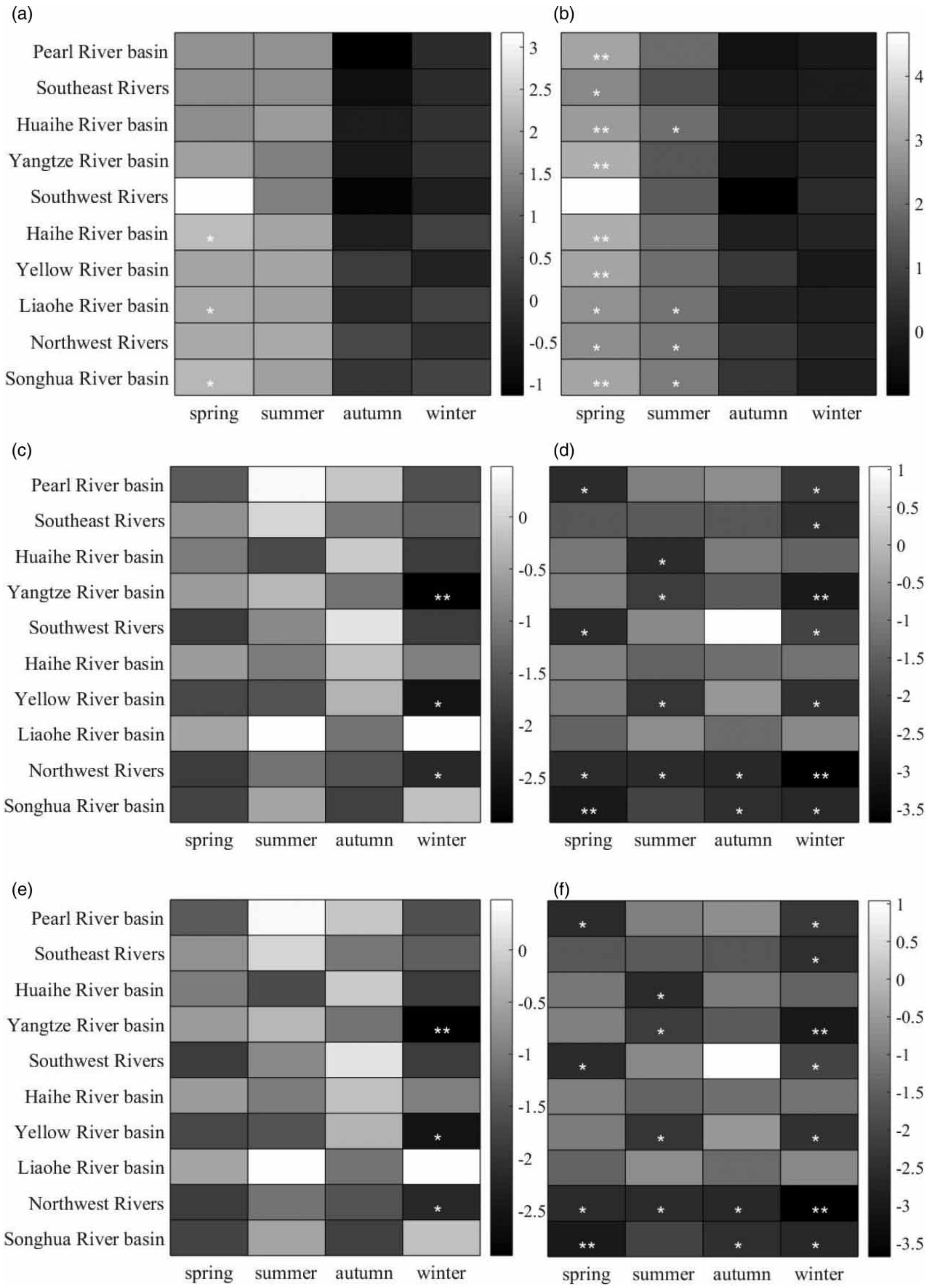

Figure 3 | Relationship between AO/NAO and seasonal EHT. *Note*: The '**' and '*' marked rectangles describe the correlation coefficient over the 0.01 or 0.05 significance level t-test, respectively. (a) ELT & AO. (b) ELT & NAO. (c) EHT & AO. (d) EHT & NAO. (e) DTR & AO. (f) DTR & NAO.

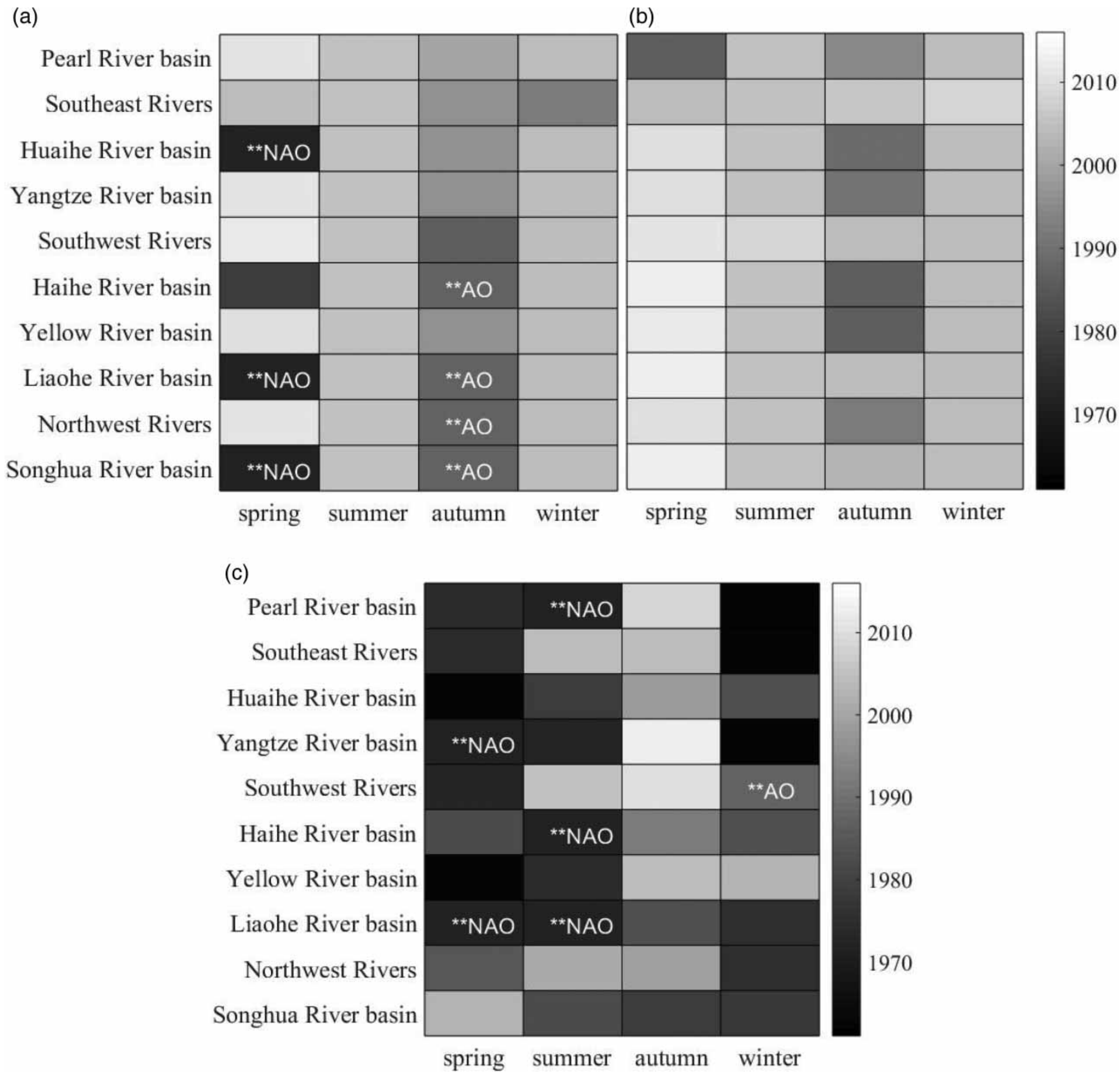

Figure 4 | Change points of ELT, EHT, and DTR in ten water resources regions. *Note*: '**NAO' and '**AO' represent that the change point is in agreement with the NAOs or AOs, respectively. (a) ELT. (b) EHT. (c) DTR.

rivers. In addition, the relationships between summer ELTs and the winter NAO in the Songhua River, Liao River, and Huai River basins and the northwestern rivers are also positive with correlation coefficients at 0.05 significance level. To further the effects of AO/NAO on ELTs, change points in them have been calculated and compared, in which those matching with AO/NAO have been shown as follows. The winter ELTs over the southeastern rivers have change points in 1992, while the change point in 1987 was observed in autumn ELTs over the northwestern rivers and the Songhua River, Liao River, and Haihe River basins. In addition, the year of 1986 is the change point for the southwestern rivers and the Pearl River basin, respectively. It is obvious that these indices almost have the same pattern as winter AOs with the change point in 1987. Moreover, the year of 1972 is the change point for the spring ELTs over the Songhua River, Liao River, and Huai River basins, and the year of 1979 was found to be the change point over the Haihe River basin and the southeastern rivers, respectively, for the spring ELTs. The NAO shifting in the year of 1972 may largely explain the change point of these spring ELTs (Zuo 2013).

The relationship between the winter AO and seasonal EHTs is nonsignificant. However, the winter NAO has a significantly positive relationship with spring EHTs. This relationship passes the 0.01 significance level test over the southwestern rivers and the Pearl River basin, while the relationships over the Songhua River, Liao River, Haihe River, and Yangtze River basins pass the 0.05 significance level test. In addition, the relationship between the autumn EHTs, the winter EHTs, and the winter NAO over the southeastern rivers are negative and pass the 0.05 significance level test. Similar to the ELT, the change points for the EHTs were also analyzed. Specifically, the Pearl River basin has a change point in 1986. For the autumn EHTs, the change points in different basins have scattered distributions from 1989 to 1992 for the northwestern rivers and the Yangtze River and Huai River basins. In addition, the year 1986 is the change point both in the Yellow River and Haihe River basins, and there is another change point in 1995 for the Pearl River basin. These are considered as having a similar pattern in the winter NAO with the change point in 1987.

In terms of the winter AO and the seasonal DTR, a negative relationship was observed for the northwestern rivers, the Yellow River, and Yangtze River basins. The correlation coefficient for the Yangtze River basin passes the 0.01 significance level test, and those of the other two pass the 0.05 significance level test. However, a negative relationship was generally found between the winter NAO and the seasonal DTR. Specifically, the spring DTRs over the Songhua River basin, the northwestern and southwestern rivers, and the Pearl River basin, as well as most winter DTRs, are negatively related to the winter NAO. In addition, the summer DTRs over the northwestern rivers and the Yellow River, Yangtze River, and Huai River basins, as well as the autumn DTRs over the Songhua River basin and the southwestern rivers, are also negatively related with the winter NAO. With respect to the change points for DTRs, the spring and summer over the Liao River basin, the spring over the Yangtze River basin, and the summer over the Haihe River and Pearl River basins shift in 1972, which lags one year behind the change point in the winter NAO. In addition, the change point for the winter DTR over the southwestern rivers occurs in 1987, which is consistent with the winter AOs.

DISCUSSION

Trend in temperature extremes

Regional warming in China has been identified. For instance, Ren & Zhai (1998) found that northern areas have greater trend in ELT both during spring and autumn. Similar results were also obtained in the present research. In addition, Zhang *et al.* (2008) documented that EHT in the downstream of the Yellow River basin appeared a significantly decreasing trend during 1955–2005, while after the current analysis, the areas with decreasing trend in summer EHT have expanded, including the northwest rivers, Haihe River, Yangtze River, Huaihe River basin, and the southeast rivers. In addition, stronger warming in winter than in summer and significantly decreasing trend in DTR concluded from the above analysis is consistent with Xu *et al.* (2013). In particular, decreasing trend in DTR of the Songhua River basin was most significant, which is consistent with Zhong *et al.* (2017). Kukal & Irmak (2016) pointed out that the significant downward trend in DTR may be caused by decrease in incoming shortwave radiation and atmospheric moisture increase. In addition, the result in GSLs lengthening, and frozen and frost days shortening, may provide a reference for agricultural prearrangements.

Linkages of AO/NAO to temperature extremes

To further the effects of AO/NAO on temperature extremes, change points in frozen and frost days and GSL were identified. The change points for frozen and frost days span over 1986–1988, which is close to the timing for the AO changes in 1987. It suggests that the change in AO is responsible for the shifting in frozen and frost days consistent with AO and NAO being strongly associated with frozen days and frost days (Table 1). In terms of the DTR, the year of 1972 is when the change point for the spring DTR occurred, which may be explained by the shifting in winter NAO with change point in 1971. It also matches that the winter NAO has a significant relationship with the seasonal DTR.

The AO is one of the dominant atmospheric circulation modes in the extratropic of the northern hemisphere, alternating between positive and negative phases (Thompson &

Table 1 | Relationship between AO/NAO and three temperature extremes on mainland China

Atmospheric circulation factors	Frozen days	Frost days	GSL
NAO	**−3.12****	**−3.47****	**3.55****
AO	**−3.06****	−2.50*	**2.77****

Note: Numbers with '−' present have negative relationship. The '**' marked bold numbers and '*' marked numbers represent the correlation coefficient calculated by Pearson correlation analysis over the 0.01 and 0.05 significance level of standard t-test, respectively.

Wallace 2000). The AO is enhanced during the winter and weakened during the summer having a profound effect on the temperatures in China by influencing the Siberian High and thereby the East Asian Winter Monsoon (Thompson & Wallace 1998, 2000; Alexander *et al.* 2006; He *et al.* 2017). Zuo (2013) has described how AO significantly influences the air temperature above 35°N over mainland China in an opposite way, and pointed out that the effects of NAO/AO on local SST (sea surface temperature) anomalies may be one of the potential pathways to influence climate over mainland China. It can explain that ELTs in the northern areas have more significant increasing trend in summertime (including summer and autumn). In combination with the above analysis, the NAO may account for the significant increasing trend in ELTs in wintertime (including winter and spring). Moreover, the winter NAO was found to have significant effects on spring EHT over mainland China, while decreasing trend was detected in EHTs in the southeastern areas. The phenomenon may be attributed to change in the NAO coupled with several other atmospheric circulations and regional elevation distribution (Beniston & Rebetez 1996; Giorgi *et al.* 1997; Feng *et al.* 2018).

Limitation of the study

The biggest limitation of the study is that only AO and NAO were selected for the attribution analysis in changes of temperature extremes, which restricts understanding in the mechanism to some extent. Another limitation is that uneven distribution of meteorological stations blocked several regional characteristics somehow. According to relevant reports, global warming, change in atmospheric circulation, SST (sea surface temperature), land use and cover, and aerosol emissions and other human activities can affect temperature extremes (Xi *et al.* 2018; Wu *et al.* 2019). In terms of how the linkages work, Li *et al.* (2012a, 2012b) identified atmospheric circulation in China is influenced by the Subtropical High, the polar vortex, the East Asian monsoon (EAM), tropical cyclones, etc. Moreover, urbanization, land use change, and other anthropogenic activities such as higher greenhouse gas emission, etc., have significant effects on temperature extremes (Sun & Wang 2008; Wang *et al.* 2010). However, the existing studies have not completely clarified the physical mechanism in the influencing mode, which needs to be further advanced in future relevant work.

CONCLUSIONS

Spatial and temporal patterns of extreme temperature indices and their relationships on both annual and seasonal scale with the winter AO/NAO over mainland China were investigated by trend analysis, and change point and correlation coefficient calculations. The conclusions are summarized as follows:

1. ELTs, EHTs, and GSLs gradually increase from north to south, while the DTR decreases from north to south. Similarly, the number of frozen and frost days also decrease from north to south.
2. Spatial discrepancy in temperature distribution over mainland China is shrinking, and temperature range is shortening. ELTs generally show significant increasing trend, particularly in winter. The increasing trends in northern basins are more significant. However, EHTs generally have inconspicuous trend, and the summer EHTs even show decreasing trend. Frozen days and frost days have significant increasing trend, while the GSL shows the opposite. In particular, DTR in Songhua River basin and the northwest rivers have significantly decreasing trend.
3. The increasing trend of ELTs in summertime for the northern areas can be mainly attributed to change in the AO, and the NAO accounts for their changes in wintertime. The insignificant decreasing trend of EHTs in the southeastern areas primarily results from the sea–land interaction, in which the NAO plays an important role, while other coupled atmospheric circulation proxies still need to be further investigated. The physical

mechanism for how these atmospheric circulations influence the climate extremes also need further explorations in future studies.

ACKNOWLEDGEMENTS

This study is financially supported by the State Key Program of National Natural Science of China (91647202). The authors declare no conflicts of interest.

SUPPLEMENTARY MATERIAL

The Supplementary Material for this paper is available online at https://dx.doi.org/10.2166/wcc.2019.302.

REFERENCES

Alexander, L. V., Zhang, X., Peterson, T. C., Caesar, J., Gleason, B., Klein-Tank, A. M. G., Haylock, M., Collins, D., Trewin, B., Rahimzadeh, F., Tagipour, A., Rupa-Kumar, K., Revadekar, J., Griffiths, G., Vincent, L., Stephenson, D. B., Burn, J., Aguilar, E., Brunet, M., Taylor, M., New, M., Zhai, P., Rusticucci, M. & Vazquez-Aguirre, J. L. 2006 Global observed changes in daily climate extremes of temperature and precipitation. *J. Geophys. Res.* **111**, D05109. doi:10.1029/2005JD006290.

Beniston, M. & Rebetez, M. 1996 Regional behavior of minimum temperatures in Switzerland for the period 1979–1993. *Theor. Appl. Climatol.* **53** (4), 231–243.

Castro-Díez, Y., Pozo-Vázquez, D., Rodrigo, F. S. & Esteban-Parra, M. J. 2002 NAO and winter temperature variability in southern Europe. *Geophys. Res. Lett.* **29** (8), 1–4.

Chan, J. C. L. & Zhou, W. 2005 PDO, ENSO and the early summer monsoon rainfall over south China. *Geophys. Res. Lett.* **32** (8), 93–114.

Chen, H. & Sun, J. 2015 Changes in climate extreme events in China associated with warming. *Int. J. Climatol.* **35** (10), 2735–2751.

Chen, Z., Chen, Y., Bai, L. & Xu, J. H. 2016 Multiscale evolution of surface air temperature in the arid region of Northwest China and its linkages to ocean oscillations. *Theor. Appl. Climatol.* **128** (3), 1–14.

Cropper, T. E. & Hanna, E. 2012 An analysis of the climate of Macaronesia, 1865–2012. *Int. J. Climatol.* **34** (3), 604–622.

Donges, J. F., Zou, Y., Marwan, N. & Kurths, J. 2009 Complex networks in climate dynamics. *Eur. Phys. J. Spec. Topics* **174** (1), 157–179.

Feng, R., Yu, R. D., Zheng, H. W. & Gan, M. 2018 Spatial and temporal variations in extreme temperature in Central Asia. *Int. J. Climatol.* **38** (Suppl. 1), e388–e400. doi:10.1002/joc.5379.

Fischer, T., Gemmer, M., Liu, L. L. & Su, B. D. 2011 Change-points in climate extremes in the Zhujiang River Basin, South China, 1961–2007. *Clim. Chang.* **110** (3–4), 783–799.

Frich, P., Alexander, L. V., Della-Marta, P., Gleason, B., Haylock, M., Klein-Tank, A. M. G. & Peterson, T. 2002 Observed coherent changes in climatic extremes during the second half of the twentieth century. *Clim. Res.* **19** (3), 193–212.

Ghorbani, M. A., Kazempour, R., Chau, K. W., Shamshirband, S. & Ghazvinei, P. T. 2018 Forecasting pan evaporation with an integrated Artificial Neural Network Quantum-behaved Particle Swarm Optimization model: a case study in Talesh, Northern Iran. *Eng. Appl. Comput. Fluid Mech.* **12** (1), 724–737.

Giorgi, F., Hurrell, J. W., Marinucci, M. R. & Beniston, M. 1997 Elevation dependency of the surface climate change signal: a model study. *J. Clim.* **10** (2), 288–296.

Grant, P. R. 2017 Evolution, climate change, and extreme events. *J. Climate* **357** (6350), 451–452.

Gruza, G., Rankova, E., Razuvaev, V. & Bulygina, O. 1999 Indicators of climate chance for the Russian Federation. *Clim. Chang.* **42** (1), 219–242.

He, S. P. & Wang, H. J. 2016 Linkage between the East Asian January temperature extremes and the preceding Arctic Oscillation. *Int. J. Climatol.* **36** (2), 1026–1032.

He, S., Gao, Y., Li, F., Wang, H. J. & He, Y. C. 2017 Impact of Arctic Oscillation on the East Asian climate: a review. *Earth Sci. Rev.* **164**, 48–62. doi:10.1016/j.earscirev.2016.10.014.

Jia, P. P., Zhuang, D. F. & Wang, Y. 2017 Impacts of temperature and precipitation on the spatialtemporal distribution of water resources in Chinese mega cities: the case of Beijing. *J. Water Climate Change* **8** (4), 593–612.

Jiang, D., Wang, K. & Li, Z. 2011 Trends of extreme precipitation events over Shandong province from 1961 to 2008. *Sci. Geogr. Sin.* **31** (9), 1118–1124.

Kukal, M. & Irmak, S. 2016 Long-term patterns of air temperatures, daily temperature range, precipitation, grass-reference evapotranspiration and aridity index in the USA great plains: Part II. Temporal trends. *J. Hydrol.* **542**, 978–1001. doi:10.1016/j.jhydrol.202016.06.008.

Lee, H. F. & Zhang, D. D. 2011 Relationship between NAO and drought disasters in northwestern China in the last millennium. *J. Arid Environ.* **75** (11), 1114–1120.

Li, Z. X., He, Y. Q., Wang, C. F., Wang, X. F., Xin, H. J., Zhang, W. & Cao, W. H. 2011 Spatial and temporal trends of temperature and precipitation during 1960–2008 at the Hengduan Mountains, China. *Quat. Int.* **236**, 127–142.

Li, Z. X., He, Y. Q., Wang, P. Y., Theakstone, W. H., An, W. L., Wang, X. F., Lu, A. G., Zhang, W. & Cao, W. H. 2012a Changes of daily climate extremes in southwestern China during 1961–2008. *Glob. Planet. Chang.* **80-81**, 255–272. doi:10.1016/j.gloplacha.2011.06.008.

Li, Z., Zheng, F. L., Liu, W. Z. & Jiang, D. J. 2012b Spatially downscaling GCMs outputs to project changes in extreme precipitation and temperature events on the Loess Plateau of China during the 21st century. *Glob. Planet. Chang.* **82–83**, 65–73.

Linderholm, H. W. 2006 Growing season changes in the last century. *Agric. Forest Meteorol.* **137** (1–2), 1–14. doi:10.1016/j.agrformet.202006.03.006.

Linderholm, H. W., Seim, A., Ou, T., Jeong, J. H., Liu, Y., Wang, X. C., Bao, G. & Folland, C. 2013 Exploring teleconnections between the summer NAO (SNAO) and climate in East Asia over the last four centuries – a tree-ring perspective. *Dendrochronologia* **31** (4), 297–310.

Liu, S. Y., Huang, S. Z., Xie, Y. Y., Huang, Q., Leng, G. Y., Hou, B. B., Zhang, Y. & Wei, X. 2018 Spatial-temporal changes of maximum and minimum temperatures in the Wei River Basin, China: changing patterns, causes and implications. *Atmos. Res.* **204**, 1–11. doi:10.1016/j.atmosres.2018.01.006.

López-Moreno, J. I., Vicente-Serrano, S. M., Morán-Tejeda, E., Lorenzo-Lacruz, J., Kenawy, A. & Beniston, M. 2011 Effects of the North Atlantic Oscillation (NAO) on combined temperature and precipitation winter modes in the Mediterranean mountains: observed relationships and projections for the 21st century. *Glob. Planet. Chang.* **77** (1–2), 62–76.

Ma, Z. G., Fu, C. B., Ren, X. B. & Yang, C. 2003 Trends of annual extreme temperature and its relationship to regional warming in Northern China. *Acta Geograph. Sin.* **58**, 11–20.

Mahmood, R. & Jia, S. F. 2017 Spatial and temporal hydro-climatic trends in the transboundary Jhelum River basin. *J. Water Climate Change* **8** (3), 423–440.

Meehl, G. A., Thomas, K., Easterling, D. R., Changnon, S., Pielke Jr., R., Changnon, D., Evans, J., Groisman, P. Y., Knutson, T. R., Kunkel, K. E., Mearns, L. O., Parmesan, C., Pulwarty, R., Root, T., Sylves, R. T., Whetton, P. & Zwiers, F. 2000 An introduction to trends in extreme weather and climate events observations, socioeconomic impacts, terrestrial ecological impacts, and model projections. *Bull. Am. Meteorol. Soc.* **81** (3), 413–416.

Mutiibwa, D., Vavrus, S. J., McAfee, S. A. & Albright, T. P. 2015 Recent spatiotemporal patterns in temperature extremes across conterminous United States. *J. Geophys. Res. Atmos.* **120** (15), 7378–7392. http://dx.doi.org/10.1002/2015JD023598.

New, M., Hewitson, B., Stephenson, D. B., Tsiga, A., Kruger, A., Manhique, A., Gomez, B., Coelho, C. A. S., Masisi, D. N., Kululanga, E., Mbambalala, E., Adesina, F., Saleh, H., Kanyanga, J., Adosi, J., Bulane, L., Fortunata, L., Mdoka, M. L. & Lajoie, R. 2006 Evidence of trends in daily climate extremes over southern and west Africa. *J. Geophys. Res.* **111**, D14102. http://dx.doi.org/10.1029/2005JD006289.

Partal, T. 2017 Multi-annual analysis and trends of the temperatures and precipitations in West Anatolia. *J. Water Climate Change* **8** (3), 456–473.

Ren, F. M. & Zhai, P. M. 1998 Study on changes of China's extreme temperatures during 1951–1990. *Sci. Atmos. Sin.* **22** (2), 217–227.

Renom, M., Rusticucci, M. & Barreiro, M. 2011 Multidecadal changes in the relationship between extreme temperature events in Uruguay and the general atmospheric circulation. *Clim. Dyn.* **37** (11–12), 2471–2480. doi:10.1007/s00382-010-0986-9.

Scaife, A. A., Folland, C. K., Alexander, L. V., Moberg, A. & Knight, J. R. 2008 European climate extremes and the North Atlantic Oscillation. *J. Clim.* **21** (1), 72–83.

Shi, J., Cui, L. L., Ma, Y., Du, H. Q. & Wen, K. M. 2018 Trends in temperature extremes and their association with circulation patterns in China during 1961–2015. *Atmos. Res.* **212**, 259–272. doi:10.1016/j.atmosres.2018.05.024.

Su, Z., Hao, Z., Yuan, F., Chen, X. & Cao, W. 2017 Spatiotemporal variability of extreme summer precipitation over the Yangtze River basin and the associations with climate patterns. *Water SA* **9** (11), 873.

Sun, G. N. & Wang, M. H. 2008 Study on relation and distribution between vegetative coverage and land degradation in inner Mongolia. *J. Arid Land Resour. Environ.* **22** (2), 140–144.

Suo, L. L., Huang, J. Y. & Tan, B. K. 2008 The influence of winter Arctic Oscillation on maximum and minimum air temperature over China in winter. *J. Trop. Meteorol.* **24** (2), 163–168.

Thompson, D. W. & Wallace, J. M. 1998 The Arctic Oscillation signature in the wintertime geopotential height and temperature fields. *Geophys. Res. Lett.* **25** (9), 1297–1300.

Thompson, D. W. J. & Wallace, J. M. 2000 Annular modes in the extratropical circulation. Part I: month-to-month variability. *J. Clim.* **13** (5), 1000–1016.

Tong, S. Q., Li, X. Q., Zhang, J. Q., Bao, Y. H., Bao, Y. B., Na, L. & Si, A. L. 2019 Spatial and temporal variability in extreme temperature and precipitation events in Inner Mongolia (China) during 1961–2017. *Sci. Total Environ.* **649**, 75–89. doi:10.1016/j.scitotenv.2018.08.262.

Waliser, D., Stern, W., Schubert, S. & Lau, W. K. M. 2003 Dynamic predictability of intraseasonal variability associated with the Asian summer monsoon. *Q. J. Roy. Meteorol. Soc.* **129** (594), 2897–2925.

Wan, S. Q., Gu, C. H., Kang, J. P., Zou, J. X., Hu, Y. L. & Xu, S. S. 2010 Monthly extreme high temperature response to atmospheric oscillation in China. *Acta Phys. Sin.* **59** (1), 676–682.

Wang, L. X., Liu, H. M. & Yang, J. 2010 Climatic change of Mu Us sandy land and its influence on vegetation coverage. *J. Nat. Resour.* **25** (12), 2030–2039.

Wang, W. C., Chau, K. W., Qiu, L. & Chen, Y. B. 2015 Improving forecasting accuracy of medium and long-term runoff using artificial neural network based on EEMD decomposition. *Environ. Res.* **139**, 46–54.

Wei, J. H. & Lin, Z. H. 2009 The leading mode of wintertime cold wave frequency in northern China during the last 42 years and its association with Arctic Oscillation. *Atmos. Oceanic Sci. Lett.* **2** (3), 130–134.

Wu, K. & Qian, W. 2015 Secular non-linear trends and multi-timescale oscillations of regional surface air temperature in eastern China. *Climate Res.* **63** (1), 19–30.

Wu, X. Y., Hao, Z. C., Hao, F. H. & Zhang, X. 2019 Variations of compound precipitation and temperature extremes in China during 1961–2014. *Sci. Total Environ.* **663**, 731–737. doi:10.1016/j.scitotenv.2019.01.366.

Xi, Y., Miao, C., Wu, J., Duan, Q., Lei, X. & Li, H. 2018 Spatiotemporal changes in extreme temperature and precipitation events in the Three-Rivers headwater region, China. *J. Geophys. Res. Atmos.* **123**, 5827–5844. doi:10.1029/2017JD028226.

Xu, W. H., Li, Q. X., Wang, X. L., Yang, S., Cao, L. J. & Feng, Y. 2013 Homogenization of Chinese daily surface air temperature and analysis of trends in the extreme temperature indices. *J. Geophys. Res. Atmos.* **118**, 9708–9720.

You, Q. L., Ren, G. Y., Fraedrich, K., Kang, S. C., Ren, Y. Y. & Wang, P. L. 2013 Winter Temperature extremes in China and their possible causes. *Int. J. Climatol.* **33**, 1444–1455.

Zhang, N., Sun, Z. B. & Zeng, G. 2008 Change of extreme temperatures in China during 1995–2005. *J. Nanjing Inst. Meteorol.* **31** (1), 123–128.

Zhang, Q., Singh, V. P., Li, J., Jiang, F. & Bai, Y. 2012 Spatio-temporal variations of precipitation extremes in Xinxiang, China. *J. Hydrol. Sci.* **434–435** (2), 7–18.

Zhong, K., Zheng, F., Wu, H., Qin, C. & Xu, X. 2017 Dynamic changes in temperature extremes and their association with atmospheric circulation patterns in the Songhua River Basin, China. *Atmos. Res.* **190**, 77–88. doi:10.1016/j.atmosres.2017.02.012.

Zhou, L. T. & Wu, R. 2010 Respective impacts of the East Asian winter monsoon and ENSO on winter rainfall in China. *J. Geophys. Res. Atmos.* **115** (D2), 107. https://doi.org/10.1029/2009JD012502.

Zuo, J. Q. 2013 *Relationship Between AO/NAO and ENSO and Their Impact on Climate Anomalies in China*. PhD dissertation, Lanzhou University, Lanzhou, China.

Zuo, J., Ren, H. L., Li, W. & Wang, L. 2016 Interdecadal variations in the relationship between the winter North Atlantic Oscillation and temperature in South-Central China. *J. Climate* **29** (20), 7477–7493.

First received 28 May 2019; accepted in revised form 16 September 2019. Available online 21 October 2019